PERGAMON

International Journal of Heat and Mass Transfer 45 (2002) 1605–1613

International Journal of HEAT and MASS TRANSFER

www.elsevier.com/locate/ijhmt

Conjugate heat transfer measurements in a non-uniformly heated circular flow channel under flow boiling conditions

Ronald D. Boyd Sr. *,[1], Penrose Cofie, Ali Ekhlassi

College of Engineering, Thermal Science Research Center, Prairie View A&M University, P.O. Box 4208, Prairie View, TX 77446-4208, USA

Received 12 April 2001; received in revised form 23 August 2001

Abstract

Plasma-facing components (PFCs) for fusion reactors and high heat flux heat sinks for electronic applications, are usually subjected to a peripherally non-uniform heat flux. The configuration under study is related to these applications and consists of a single-side heated circular-like cross-section test section (TS) with a circular coolant channel bored through the center. The TS has a heated length of 180.0 mm and has 10.0 and 30.0 mm inside and outside diameters, respectively. It was subjected to a constant heat flux on one side only, and the remaining half of the circumferential surface is not exposed to a heat flux. The inlet channel water temperature was held constant at 26.0 °C, the exit pressure was maintained at 0.207 MPa, and the mass velocity was 0.59 Mg/m^2 s. The results consist of three-dimensional TS wall temperature distributions and a clear display of both CHF and post-CHF for this single-side heated configuration. These results are very encouraging in that they are among the first full set of truly three-dimensional TS wall temperature measurements for a one-side heated (OSH) flow channel which contains the effect of conjugate heat transfer for turbulent, subcooled flow boiling.

Keywords: Three-dimensional; Subcooled flow boiling; Single-side heating

1. Introduction

Conjugate heat transfer modeling [1,2] has proved useful in forming baselines and identifying important parameters affecting peaking factors (PFs) and data reduction for the spectrum of high heat fluxes found in a wide variety of applications. For various applications requiring different fluids, the results show the following:

1. the coexistence of three flow boiling regimes inside an one-side heated (OSH) circular geometry (for water only),
2. the correlational dependence of the inside wall heat flux and temperature (fluid independent) and
3. inaccuracies that could arise in some data reduction procedures (fluid independent).

However, for plasma-facing component (PFC) applications in fusion reactors, work to expand conjugate heat transfer analyses from simple circular and complex geometries to PFC geometries is still needed for consistently predicting PFs for OSH channels.

The configuration under study consists of a non-uniformly heated cylindrical-like test section (TS) with a circular coolant channel bored through the center. The theoretical or idealization of the cylindrical-like TS would be a circular cylinder with half (−90° to +90°) of its outside boundary subjected to a uniform heat flux and the remaining half insulated. The outside diameter of the cylindrical-like TS was 30.0 mm and its length was 200.0 mm. The actual directly heated length (L) was 180.0 mm. The inside diameter of the flow channel was 10.0 mm. Water was the coolant. The inlet water temperature can be set at any level in the range from 26.0 to 130.0 °C and the exit pressure can be set at any level in the range from 0.2 to 4.0 MPa. Thermocouples were

* Corresponding author. Tel.: +1-936-857-4811; fax: +1-936-857-2325.

E-mail address: ronald_boyd@pvamu.edu (R.D. Boyd Sr.).

[1] Distinguished Professor of Mechanical Engineering and Honeywell Endowed Professor of Engineering.

0017-9310/02/$ - see front matter
PII: S0017-9310(01)00278-2

Nomenclature

A_H	outside heated surface area $= 5.0tL$ (m^2)
L	heated length of the directly heated coolant channel (m)
L_i	unheated inlet length of the directly heated TS (m)
L_o	unheated exit length of the directly heated TS (m)
q_o	outside net incident single-side heat flux, which is computed as the ratio of the net incident power to A_H (kW/m^2)
r	radial coordinate (m)
r_i	inside radius of coolant channel (m)
r_o	outside radius of coolant channel (m)
t	width of one of the five heaters (m)
T_w	local wall temperature (°C)
Z	axial coordinate or measurement location (m)
Z_j	axial coordinate location for axial sections A–A ($Z = Z_4$), B–B ($Z = Z_3$), C–C ($Z = Z_2$), and D–D ($Z = Z_1$), where $j = 1, 2, 3$, or 4 (see Fig. 1 for the numerical dimensions)

Greek symbol

ϕ	circumferential coordinate with the origin at the heated part of the axis of symmetry (°)

placed at 48 locations inside the solid cylindrical-like or monoblock TS. For each of four axial stations, three thermocouples were embedded at four circumferential locations (0°, 45°, 135°, and 180°, where 0° corresponds to that portion of the axis of symmetry close to the heated surface) in the wall of the TS. Finally, the mass velocity can be set at any level in the range from 0.5 to 10.0 Mg/m^2 s.

The mass velocity, exit pressure, and inlet water temperature used for the present case were 0.59 Mg/m^2 s, 0.207 MPa ($T_{sat} = 121.3$ °C) and 26.0 °C, respectively. Type-*J* thermocouples were used and calibrated to within ±0.1 °C with a precision calibrator. For these conditions, the basic fluid flow is a turbulent ($Re = 6900$) and highly developing flow with a reciprocal Graetz number (Gz^{-1}) of 4.5×10^{-4}. A detail description of the test facility, experimental, and measurement details are given elsewhere by Boyd et al. [3].

International efforts are vigorously proceeding in the investigation of heat transfer and related CHF in OSH flow channels. Some examples of recent one-side heating efforts include:

(1) the international round-robin monoblock CHF swirl-flow tests by Youchison et al. [4];
(2) CHF in multiple square channels by Akiba et al. [5];
(3) CHF comparison of an attached-fin hypervapotron and porous coated surface by Youchison et al. [6];
(4) CHF enhancements due to wire inserts by Youchison et al. [7];
(5) post-CHF with and without swirl flow in a monoblock by Marshall [8];
(6) CHF JAERI data base compilation by Boscary et al. [9,10];
(7) post-CHF enhancement factors by Marshall et al. [11];
(8) CHF peaking factor empirical correlations by Inasaka and Nariari [12], and Akiba et al. [13];
(9) CHF correlation modification to account for peripheral non-uniform heating by Celata, et al. [14];
(10) comparison of one-side heating with uniform heating by Boyd [15];
(11) single- and two-phase subcooled flow boiling heat transfer in smooth and swirl tubes by Araki et al. [16];
(12) smooth tube heat transfer, CHF and post-CHF by Becker et al. [17]; and
(13) turbulent heat transfer analysis by Gartner et al. [18].

2. TS

The TSs were fabricated from Type AL-15 Glidcop Grade Copper. A detailed description of the TS is shown in Fig. 1. The overall length of the TS, including the inlet and outlet reduced diameter sections, is 328.0 mm. The main section of the TS (available for heating) is 200.0 mm long with a nominal outside diameter of 30.0 mm and an inside diameter of 10.0 mm. For these tests, the actual heated length, L, was 180.0 mm. In Fig. 1, both isometric and longitudinal side views are shown. The flow channel inlet and exit are indicated in the latter view. Also shown in the latter view are four axial stations labeled A–A, B–B, C–C, and D–D, which are axial locations where thermocouple (TC) wells exist for local in-depth wall temperature measurements. The purpose of the four axial locations is to obtain an estimate of the axial distribution of the TS wall temperature for a given applied heat flux. Since the geometry of the TC wells is identical at all four primary axial stations, a detail description will be given for only one axial station. For example, the A–A axial station in Fig. 1 has twelve (12) TC wells. Ten (10) of the TC wells are in plane A1; and, one TC well is in plane A2 and another TC well is in plane A3. Planes A2 and A3 are axially displaced upstream from plane A1 by 2.0 and 4.0 mm, respectively.

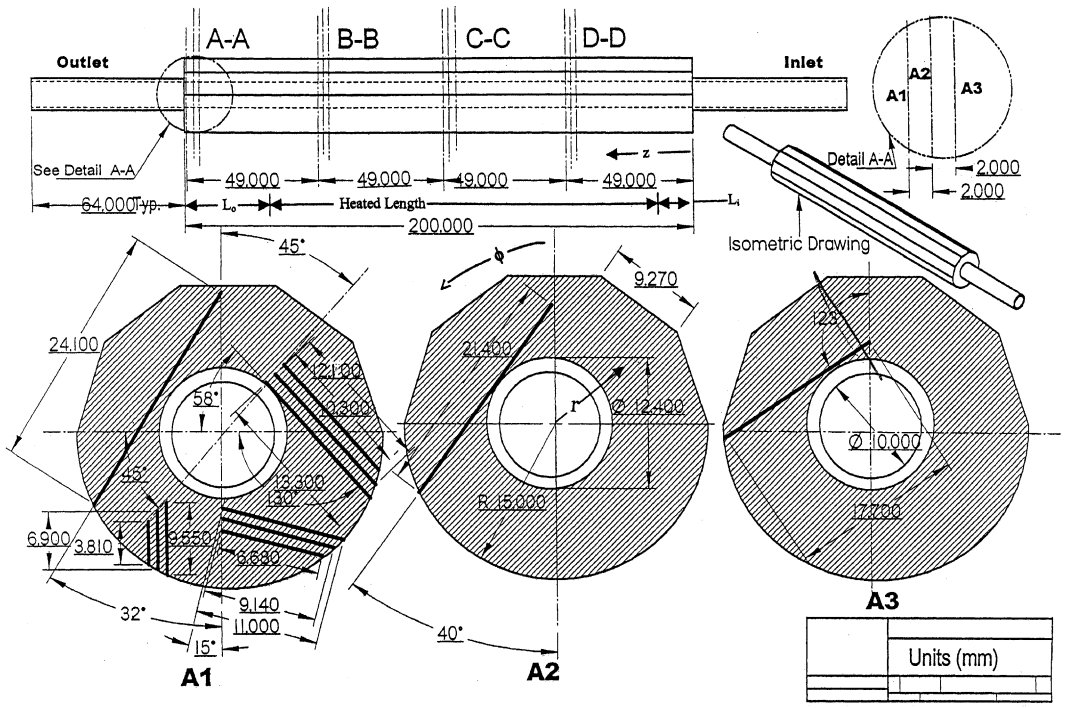

Fig. 1. TS used for local temperature and heat transfer measurements. Water flows through the 10.0 mm diameter channel. The TC wells are the solid black lines with specified lengths and angles. The outer concentric circle around the 10.0 mm inner diameter channel should not appear in the shown sections but has been added to show the outside diameter of the channel near the inlet and exit. *Note*: At $\phi = 0°$, the single TC shown in plane A3 should be switched with the corresponding TC in plane A1.

Finally, the lengths L_i and L_o shown in Fig. 1 are variable lengths whose sum must equal 20.0 mm for a given experimental setup.

The TCs at station A–A will give both radial and circumferential distributions of the local wall temperature. Hence, a combination of all axial stations will produce a three-dimensional distribution of the TS local wall temperature as a function of the applied heat flux and the water flow regime which will vary from single-phase at the TS inlet to subcooled pre- or post-CHF at the exit. The applied heat flux comes from a 350.0 kW DC power supply which provides resistive heating to the TS via five (5), grade G-20 graphite flat heaters which are shown in Figs. 2(a) and (b) and each placed over a 1.0 mm thick aluminum nitride layer which in turn rests on each of the five (5) flat sides of the TS shown in Fig. 1. The power supply provides power to the heater elements (see Fig. 2) in the experimental setup through a copper bus duct/cabling (bus bar) system [3].

3. Results

Robust PFC designs must be based on accurate three-dimensional conjugate flow boiling analyses and optimizations of the PFC local wall temperature and hence on the local flow boiling regime variations. Such analyses must have three-dimensional data as a basis for comparison, assessment, and flow boiling correlation adaptation for localize boiling. As an initial part of an effort to begin to provide such data, selected results are presented for the above noted conditions for the: (1) three-dimensional variations of the wall temperature as functions of the circumferential (ϕ), radial (r), and axial (Z) coordinates; (2) outside steady-state heat flux as a function of the local wall temperature; and (3) occurrence of pre- and post-CHF. The outside net incident heat flux relationship with the locally measured wall temperature will be discussed first.

3.1. Outside heat flux/wall temperature relationship

Results are presented here which show the relationship, at different radii, between the outside heat flux and the local wall temperature. Although not identical, this relationship between q_o and T_w would be directly related to the two-dimensional local boiling curve if the radius at which this relationship was considered was equal to the inside radius of the flow channel. This work will eventually lead to the latter.

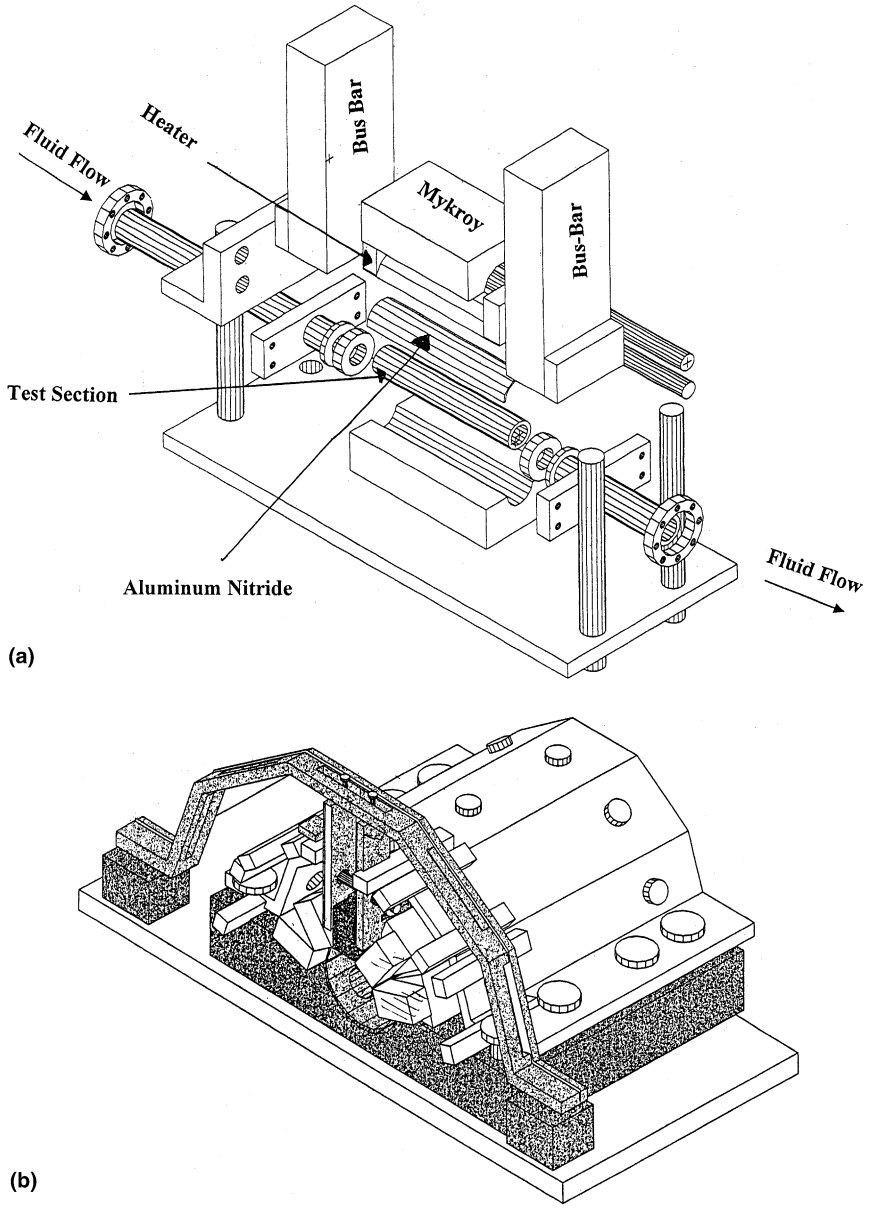

Fig. 2. (a) High heat flux TS conceptual assembly. The actual TS has five pairs of bus bar connections to five heater segments (see Fig. 2(b)). (b) TS assembly with heaters and conceptual holding fixture (see Fig. 1 and 2(a) for component labeling and details).

The relationship between the steady-state, net incident outside wall heat flux and the locally measured TS wall temperature is presented in Fig. 3 and applies for the following conditions: (1) the 180.0 mm ($= L$) heater placed asymmetrically along the axial 200.00 mm TS length, with a 4.0 mm ($= L_o$) unheated length at the downstream end of the TS, and a 16.0 mm ($= L_i$) unheated length at the upstream end of the TS; (2) $\phi = 0.0°$ at the heated side of the axis of symmetry; (3) axial locations of $Z = 143.0$, 145.0, and 147.00 mm (nominally, $Z = Z_3 = 147.0$ mm axial station); and (4) radii of 12.191, 9.881, and 8.057 mm, respectively. For the results reported below, the test conditions used for the mass velocity, and exit pressure were 0.59 Mg/m^2 s, and 0.207 MPa ($T_{sat} = 121.3$ °C), respectively.

The curves in Fig. 3 are complete in that they not only show evidence of an influence from the three basic subcooled flow boiling regimes prior to critical heat flux (CHF) (single-phase, partially nucleate boiling, and fully developed flow boiling); but, an apparent local CHF

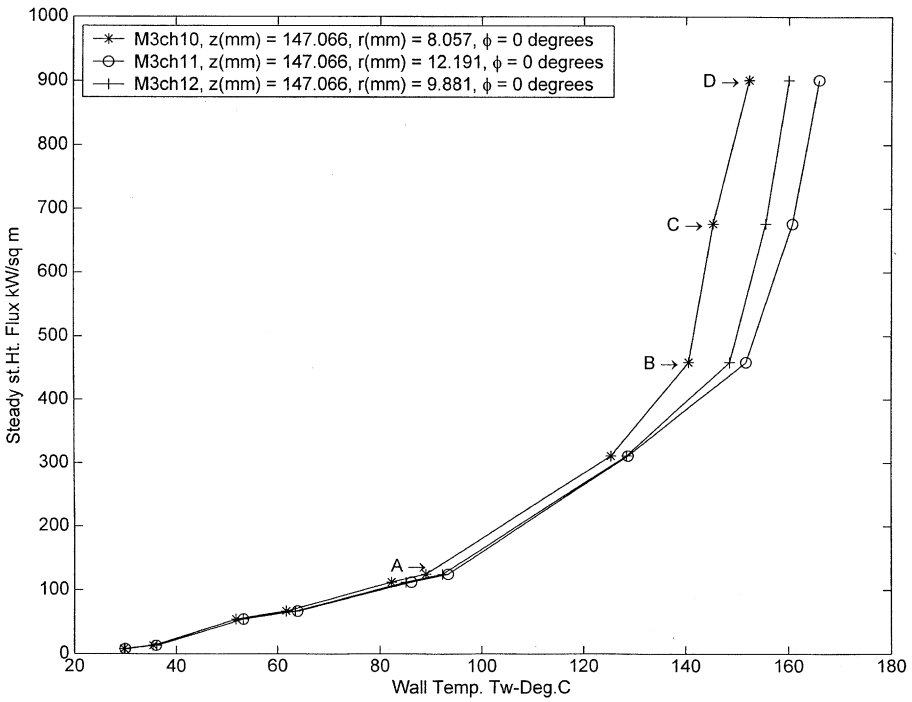

Fig. 3. Steady-state net incident heat flux as a function of the local flow channel wall temperature at $\phi = 0.0°$ and for specified axial locations (near $Z = Z_3 = 147.0$ mm) and heaters asymmetrically placed with respect to the axial direction with $L_o = 4.0$ mm and $L_i = 16.0$ mm of unheated flow channel downstream and upstream of the heaters, respectively.

occurred and is displayed near point "C" in Fig. 3 between the right-most pair of data points on the curve which corresponds to the smallest radius ($r = 8.057$ mm) with the asterisk ($*$) data points. For each curve (or radial coordinate) shown in Fig. 3, the six left-most data points show the relationship when single-phase convection exists in the flow channel; i.e., up to point "A". Beyond point "A" for each radius, the slope of each curve changes-denoting an onset of partial nucleate boiling which extends up to point "B". Finally and beyond point "B" (from left to right), one observes a progressive increase of the slope of the q_o vs T_w curves in Fig. 3 as the radius decreases or as the inside fluid–solid boundary is approached. This denotes the region of fully developed nucleate flow boiling in the flow channel and extends to point "C". The occurrence of CHF is denoted by a decrease in the slope of the left-most curve with asterisk ($*$) data points which corresponds to the smallest radius shown (8.057 mm). The reduction in the slope at the upper part of this curve in Fig. 3 suggests a stable entry into the local post-CHF regime at $\phi = 0.0°$ and $Z = Z_3 = 147.0$ mm occurred and is displayed between points "C" and "D". As the heat flux was increased above that at point "C", a loud hammer-like sound also began. The normal temperature escalation, which accompanies CHF in uniformly heated tubes, is absent due to the single-side heated flow channel and the resulting three-dimensional conjugate heat transfer (which is absent in the uniformly heated cases). This escalation may occur when a global CHF is reached [4].

3.2. Local three-dimensional variations

The circumferential variations in the channel wall temperature are presented in Figs. 4(a) and (b) for seven levels of the outside, single-side heat flux, q_o. Figs. 4(a) and (b) show such variations close to the inside fluid–solid boundary and the outside (partially heated) boundaries, respectively. Comparing the two sets of plots, one observes two very different circumferential wall temperature variations near the two boundaries. Since there are only four circumferential locations for each set of measurements, these distributions will not show the exact local circumferential slopes but the quantitative trends at the four locations are evident. As one would expect, the wall temperature approaches the fluid temperature in Fig. 4(a) (near the fluid/solid boundary) as approaches 180.0°. However, the locus of the data in Fig. 4(b) (near the outside partially heated boundary) displays approximately the correct boundary condition of a zero circumferential temperature gradient

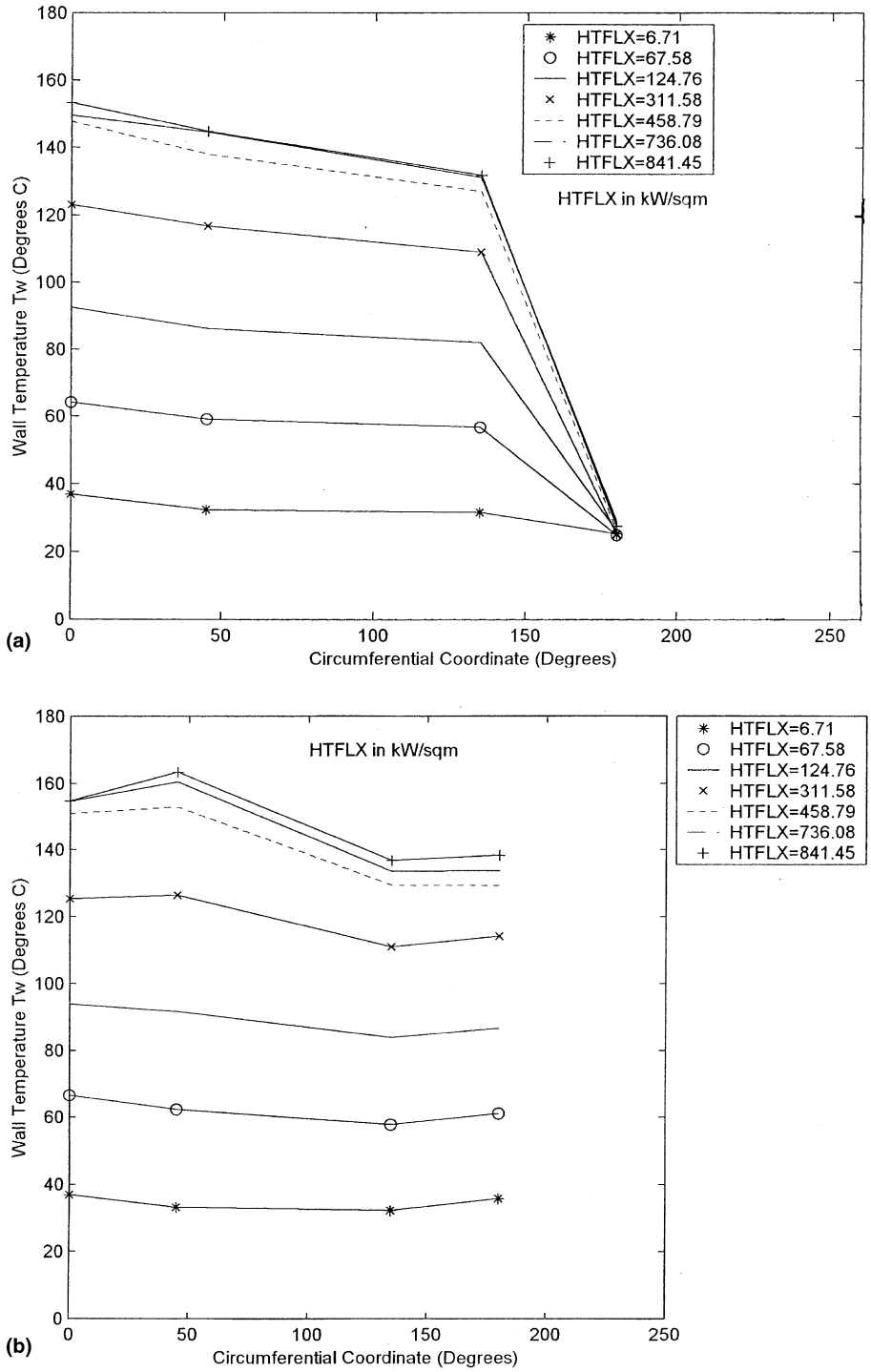

Fig. 4. (a) Circumferential wall temperature profile from the thermocouples nearest to the fluid/solid boundary as a function of net incident heat flux, at $Z = Z_4 = 196.0$ mm ($L_o = 4.0$ mm, and $L_i = 16.0$ mm). (b) Circumferential wall temperature profile from the thermocouples nearest to the heated boundary (i.e., away from the fluid/solid boundary) as a function of the net incident heat flux ($L_o = 4.0$ mm, and $L_i = 16.0$ mm).

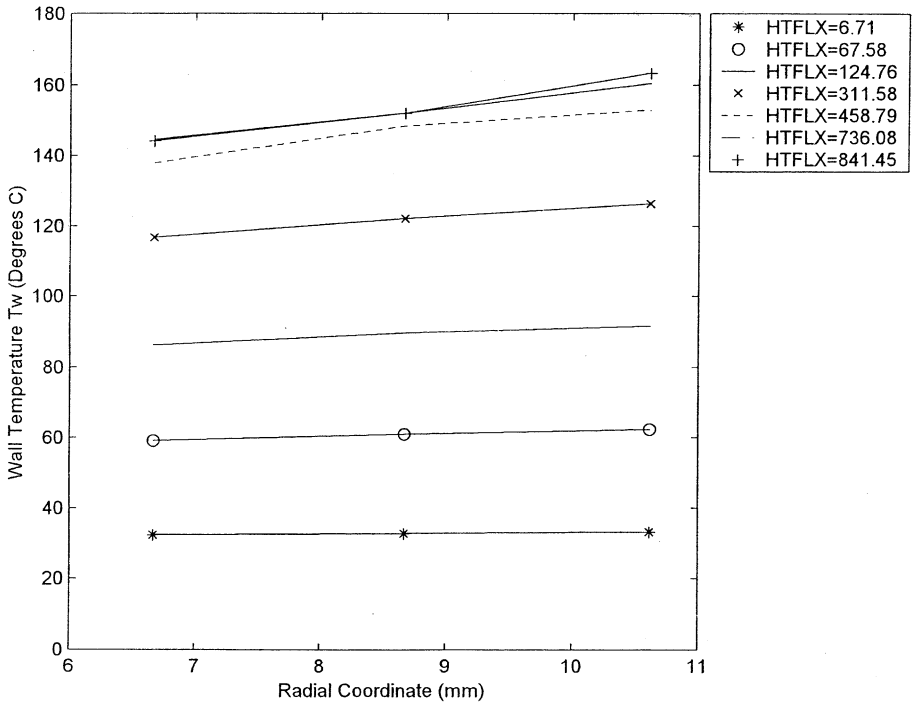

Fig. 5. Radial wall temperature profile for the flow channel at $\phi = 45.0°$ and $Z = Z_4 = 196.0$ mm as a function of the net incident heat flux ($L_o = 4.0$ mm, and $L_i = 16.0$ mm).

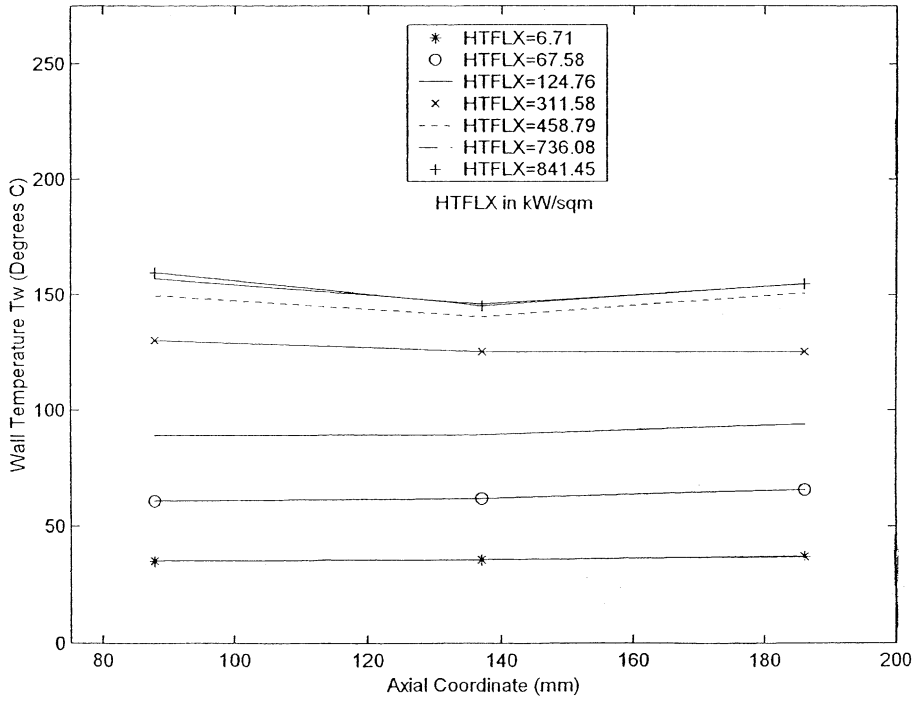

Fig. 6. Axial wall temperature profiles from the TCs at $\phi = 0.0°$, and $r = 12.191$ mm (close to the heated boundary) as a function of the net incident heat flux ($L_o = 4.0$ mm, and $L_i = 16.0$ mm).

as ϕ approaches 180.0° but differs (as it should) from the profile near the fluid/solid boundary. In both cases, the temperature is almost constant between $\phi = 45.0$ and 135.0°. This is due to the relatively large thickness of the TS. For smaller TS wall thicknesses, the variation would be greater [15]. In the limit of ϕ approaching 180.0° in Fig. 4(b), the wall temperature is well above the fluid temperature and increases as q_o increases.

Fig. 5 displays the radial temperature profiles at $\phi = 45.0°$ and shows small variations with respect to r and some values of ϕ. This is of course contrasted with larger radial variations as displayed by comparing Figs. 4(a) and (b) at other values of ϕ. These radial temperature profiles may be useful in estimating the local heat flux and wall temperature on the inside flow channel surface.

Finally, Fig. 6 shows the remaining portion of the variations via the axial wall temperature profiles which include the three downstream-most axial stations. For this experiment, the heater length (L) was 180.0 mm long (in the axial direction) and was placed asymmetrically on the TS (200.00 mm long). There was 16.0 mm ($= L_i$) of unheated (i.e., directly unheated) TS upstream of the heater and near the inlet, and 4.0 mm ($= L_o$) of unheated (i.e., directly unheated) TS downstream of the heater near the outlet. This resulted in the downstream portion of the heater being at the same downstream axial location as the TC in plane A1 of Fig. 1. As a result, the TCs at the downstream most axial location are in the same axial plane as the downstream end of the heater. The curves shown in Fig. 6 are for TS locations along the heated portion of the axis of symmetry ($\phi = 0.0°$) and close to the heated boundary ($r = 12.191$ mm). This axial wall temperature profile along the heated boundary and at $\phi = 0.0°$ shows that the wall temperature in the axial direction decreases (see Fig. 6) at higher powers due to the heat removal effect of the subcooled water flowing in the channel. However for the same value of ϕ ($= 0°$) but close to the fluid-channel wall boundary, additional profiles reveal a steady increase in the wall temperature at most power levels. Although small, axial variations occurred at all power levels. These variations would increase for TS wall and prototypic PFC substrate thicknesses smaller than the 10.0 mm nominal value for the present case.

4. Conclusions

The optimized design of OSH plasma-facing components (PFCs) and electronic heat sinks is dependent on knowing the local distribution of inside wall heat flux in the flow channels. The local inside wall heat flux can be obtain from selectively chosen local wall temperatures close to the inside boundary of the flow channel. To this end, three-dimensional thermal measurements for a OSH cylindrical-like TS were made and show:

1. the three-dimensional variation of the wall temperature close to both the heated and fluid–solid surface boundaries, and
2. the occurrence of local CHF and local post-CHF.

These results are very encouraging in that they:

1. are among the first full set of truly three-dimensional TS wall temperature measurements for OSH flow channels which contain the effect of conjugate heat transfer from turbulent, subcooled flow boiling;
2. clearly show the occurrence of CHF and post-CHF as well as two-dimensional boiling curve-related conjugate data;
3. provide a unique two-phase, turbulent, flow boiling data base for OSH flow channels which can be used for comparisons with future computational fluid dynamic and heat transfer predictions; and
4. contains the basis for extending the work of Marshall [2] in developing unified CHF and subcooled flow boiling curve correlations for OSH geometries.

Acknowledgements

The authors are appreciative to the Department of Energy (DOE) for its support of this work under contract # DEFGO3-97ER54452. The authors are also appreciative to Mrs. Vivian Pope, Mr. Qing-Yuan Li, and the Thermal Science Research Center personnel for supporting many aspect of this work. Finally, the authors are appreciative to Marcella Strahan – a raising "star"– for her contributions.

References

[1] R.D. Boyd, Single-side conduction modeling for high heat flux coolant channels, Fusion Technol. 35 (1999) 8–16.
[2] T.D. Marshall, D.L. Youchison, L.C. Cadwallader, Modeling the Nukiyama curve for water-cooled fusion divertor channels, Fusion Technol. 35 (2001) 8–16.
[3] R.D. Boyd, P. Cofie, Q.Y. Li, A. Ekhlassi, A new facility for measurements of three-dimensional, local subcooled flow boiling heat flux and related critical heat flux, in: International Mechanical Engineering Congress and Exposition (IMECE), American Society of Mechanical Engineering, HTD-866-4, Orlando, FL, November 5–10, 2000, pp. 199–208.
[4] D.L. Youchison, J. Schlosser, F. Escourbiac, K. Ezato, M. Akiba, C.B. Baxi, Round robin CHF testing of an ITER vertical target swirl tube, in: 18th IEEE/NPSS Symposium on Fusion Engineering, Albuquerque, NM, 1999, pp. 385–387.
[5] M. Akiba, K. Ezato, K. Sato, S. Suzuki, T. Hatano, Development of high heat flux components in JAERI, in: 18th IEEE/NPSS Symposium on Fusion Engineering, Albuquerque, NM, 1999, pp. 381–384.

[6] D.L. Youchison, R.E. Nygren, S. Griegoriev, D.E. Driemeyer, CHF comparison of an attached-fin hypervapotron and porous-coated channels, in: 18th IEEE/NPSS Symposium on Fusion Engineering, Albuquerque, NM, 1999, pp. 388–391.
[7] D.L. Youchison, C.H. Cadden, D.E. Driemeyer, G.W. Wille, Evaluation of helical wire inserts for CHF enhancement, in: 18th IEEE/NPSS Symposium on Fusion Engineering, Albuquerque, NM, 1999, pp. 119–122.
[8] T. Marshall, Experimental examination of the post-critical heat flux and loss of flow accident phenomena for prototypical ITER divertor channels, Ph.D. thesis, Rensselaer Polytechnic Institute, Troy, NY, 1998.
[9] J. Boscary, M. Araki, M. Akiba, Critical heat flux database of JAERI for high heat flux components for fusion applications, JAERI-Data/Code 97-037, Japan Atomic Energy Research Institute, 1997.
[10] J. Boscary, M. Araki, M. Akiba, Analysis of the JAERI critical heat flux data base for fusion application, JAERI-Data/Code 97-037, Japan Atomic Energy Research Institute, 1997.
[11] T.D. Marshall, R.D. Watson, J.M. McDonald, D.L. Youchison, Experimental investigation of post-CHF enhancement factor for a prototypical ITER divertor plate with water coolant, Symp. Fusion Eng. IEEE (1995) 206–209.
[12] R. Inasaka, H. Nariari, Critical heat flux of subcooled flow boiling in swirl tubes relevant to high-heat-flux components, Fusion Technol. 29 (1996) 487.
[13] M. Akiba, et al., Experiments on heat transfer of smooth and swirl tubes under one-sided heating conditions, in: Presented at the US/Japan Workshop, Q182, on Helium-Cooled High Heat Flux Components Design, General Atomics Corporation, San Diego, CA, 1994.
[14] G.P. Celata, M. Cumo, A. Mariani, A mechanistic model for the prediction of water-subcooled-flow-boiling critical heat flux at high liquid velocity and subcooling, Fusion Technol. 29 (4) (1996) 499.
[15] R.D. Boyd, Similarities and differences between single-side and uniform heating for fusion applications – I: Uniform heat flux, Fusion Technol. 25 (1994) 411–418.
[16] M. Araki, et al., Experiment on heat transfer of the smooth and the swirl tubes under one-side heating conditions, Department of Fusion Engineering Research, Japan Atomic Energy Research Institute (JAERI) Report, 1994.
[17] K.M. Becker et al., Heat transfer in an evaporator tube with circumferentially non-uniform heating, Int. J. Multiphase Flow 14 (5) (1988) 575–586.
[18] D. Gärtner et al., Turbulent heat transfer in a circular tube with circumferentially varying thermal boundary conditions, Int. J. Heat Mass Transfer 17 (1974) 1003–1018.